processes

MDPI

Article

Promising Porous Carbon Material Derived from Argan Paste Cake by KOH Activation, for Paracetamol Removal

El Habib Yahia [1], El Khalil Cherif [2,3,4,*], Mohammed Ouzzine [5], Abdellah Touijer [6], Franco Coren [3] and Mohamed Saidi [1]

[1] Laboratory of LAMSE, Faculty of Sciences and Techniques of Tangier, P.O. Box 416, Tangier 90000, Morocco; elhabib.yahia@uae.ac.ma (E.H.Y.); msaidi@uae.ac.ma (M.S.)
[2] Institute for Systems and Robotics, Instituto Superior Técnico, University of Lisbon, 1649-004 Lisbon, Portugal
[3] National Institute of Oceanography and Applied Geophysics (OGS), Centre for Management of Maritime Infrastructure (CGN), Borgo Grotta Gigante 42/C, Sgonico, 34010 Trieste, Italy; fcoren@ogs.it
[4] MARETEC—Marine, Environment and Technology Center, Instituto Superior Tecnico, Universidade de Lisboa, Av. Rovisco Pais 1, 1049-001 Lisboa, Portugal
[5] ERSIC Research Group, Department of Chemistry, Polydisciplinary Faculty, University of Sultan Moulay Slimane, Béni-Mellal 23000, Morocco; mohamed.ouzzine@usms.ma
[6] Department of Chemistry, Faculty of Sciences, Ibn Tofail University, Kenitra 14000, Morocco; abdellah.touijer@uit.ac.ma
* Correspondence: c.elkhalil@uae.ac.ma

Abstract: This study focuses on the preparation and characterization of activated carbon derived from Argan paste cake through carbonization at 300 °C followed by activation at 800 °C, utilizing KOH as the activation agent with a ratio of 1:1. The objective of this research is to compare the adsorption capacity of the obtained sample, referred to as APC-300-800, with a commercially available granular activated carbon (GAC) purchased from Aquasorb. The preparation involved various characterization techniques such as BET (Brunauer–Emmett–Teller) analysis, XRD (X-ray diffraction), and SEM (scanning electron microscopy). BET analysis revealed that APC-300-800 exhibited a high surface area of 1937 m^2/g. Subsequently, adsorption tests were conducted, leading to the observation that APC-300-800 conforms to the second pseudo-order kinetic model, and the adsorption of paracetamol can be accurately described by the Dubinin–Radushkevich isotherm model, exhibiting an R^2 value of 0.89665. The maximum adsorption capacity of paracetamol on APC-300-800, as determined by the Langmuir model, was found to be 344.82 mg/g. Additionally, thermodynamic studies revealed that the adsorption process on APC-300-800 was primarily governed by physisorption, while for GAC, it was attributed to chemisorption. These findings highlight the potential of APC-300-800 as an efficient adsorbent for water treatment applications, showcasing its favorable adsorption characteristics compared to commercially available alternatives.

Keywords: activated carbon; adsorption; paracetamol; granular activated carbon (GAC); Argan paste cake; comparative study

Citation: Yahia, E.H.; Cherif, E.K.; Ouzzine, M.; Touijer, A.; Coren, F.; Saidi, M. Promising Porous Carbon Material Derived from Argan Paste Cake by KOH Activation, for Paracetamol Removal. *Processes* **2023**, *11*, 2078. https://doi.org/10.3390/pr11072078

Academic Editor: Wen-Tien Tsai

Received: 14 June 2023
Revised: 6 July 2023
Accepted: 10 July 2023
Published: 12 July 2023

1. Introduction

With the emergence of accurate and sensitive instrumental chemical analysis techniques, it has become evident that numerous emerging contaminants (ECs) are present in environmental systems at low concentrations [1]. Pharmaceuticals have gained significant attention and are currently among the contaminants that are extensively researched. This heightened interest is evident from the abundance of highly regarded publications dedicated to the topic. The reason behind this interest is quite clear, as pharmaceuticals exhibit persistence in the environment and are widely utilized on a daily basis [2].

Analgesics and nonsteroidal anti-inflammatory drugs (NSAIDs) are predominantly identified as one of the primary xenobiotics found in soil, sediments, and, alarmingly, even

in drinking water sources. Unfortunately, the predictions concerning this matter are far from optimistic, largely due to the substantial annual production of NSAIDs, which hovers around several kilotons [3].

Paracetamol, recognized as a highly effective analgesic and antipyretic, holds a prominent position among the widely used medications. It is accessible both as a standalone ingredient and in combination with other components, and can be obtained either through prescriptions or over-the-counter (OTC) options [4].

While paracetamol offers therapeutic advantages, it is unfortunately recognized as a prevalent cause of poisoning worldwide. Hepatotoxicity can occur due to excessive usage, as approximately 5–10% of paracetamol is transformed by cytochrome in liver microsomes into N-acetyl-para-benzoquinone imine (NAPQI). The surplus of NAPQI leads to increased oxidative stress and mitochondrial dysfunction [5,6].

The Food and Drug Administration (FDA) of the United States emphasizes the importance of adhering to the recommended maximum dose and advises against exceeding 4000 mg as the daily limit [7]. However, as a result of widespread utilization, paracetamol consistently enters drinking water sources through its discharge into municipal wastewater, subsequently leading to contamination of nearby aquatic ecosystems, surface water, and groundwater.

Ecotoxicologists have raised concerns about the presence of pharmaceutical residues in aquatic environments and their potential long-term toxic effects. However, studying these effects is challenging due to the relatively short time period that these substances have been in the environment. Various studies have examined the microbiomes of wastewater, particularly from hospitals, and have found an abundance of anaerobic microorganisms associated with pathogenic threats, including Bifidobacteriales, Bacteroidales, and Clostridiales. Additionally, compared to other locations, hospital wastewater contains microorganisms with higher levels of antimicrobial and antibiotic resistance genes, posing a significant concern. Analysis of the mycobiomes in hospital wastewater has also revealed the presence of opportunistic phyla such as Mycosphaerella, Drechslera, Candida, and Cyphellophora. The potential for these microorganisms to acquire antibiotic resistance is alarming and could have significant implications for global health [8].

Many treatments alone prove insufficient in completely eliminating such contaminants, leaving a considerable number of them unaffected even after undergoing the treatment process, including coagulation–flocculation [9], aerobic degradation [10], ozonation [11], electrolysis [12], photo-Fenton process [13], and filtration with nanomembranes [14]. Given this scenario, it becomes imperative to devise selective methods that exhibit efficacy even when dealing with minute quantities of pollutants. Among the plethora of techniques employed in the treatment of wastewater, adsorption stands out as a highly efficient and promising approach. This widely adopted method boasts numerous advantages, including its affordability, straightforward operation and implementation, effectiveness at extremely low concentrations, and potential for regeneration and reuse, as well as the ability to utilize adsorbent materials from diverse sources. Previous studies have employed conventional water treatment methods to effectively eliminate NSAIDs from both surface and drinking water, as documented in the literature. However, Soltani et al. [15] examined the efficacy of synergistically employing catalytic decomposition and ultrasonic degradation techniques for the elimination of these compounds. The research findings revealed that the integration of stone waste (in powder form) enhanced the pore volume and specific surface area of the ZnO catalyst. As a result, a significant improvement in the degradation efficiency of paracetamol was achieved, demonstrating an outstanding outcome of approximately 98.1%. Mirzaee et al. [16] examined the electrochemical degradation of paracetamol under ultrasonic conditions. Their study showed that utilizing an iron anode in a modified hybrid process resulted in a degradation potential of over 60%. Although the catalytic and electrochemical methods exhibit higher efficiency compared to individual processes, it is important to note that they have inherent limitations and are generally more suitable for specific treatment processes and applications with lower volumes. Moreover,

conventional 2D electrochemical reactors suffer from low mass transfer, which leads to oxidation/reduction of compounds only at the surface of the electrode, thereby increasing energy consumption [17]. Moreover, wastewater typically contains chlorides, which can be converted to chlorine (Cl_2) and hypochlorites ($HOCl/OCl^-$) [18] through oxidation. These substances have the ability to react with organic materials and generate chlorinated derivatives that are hazardous and long-lasting pollutants. In contrast, the adsorption method is more discriminating as it offers flexibility in design, ease of operation, and simplicity, and it does not require specialized personnel [19].

Granular and powdered activated carbons (GACs and PACs) represent advanced treatment technologies for micropollutant removal, based on their advantages of low cost, large surface area, easy regeneration, availability, and hydrophobicity, and in this context lignocellulose biomass is gaining a lot of interest as a source for activated carbon [20].

For a considerable period of time, the use of adsorbents derived from biological species has been applied in the removal of various types of contaminants [21,22]. One of these adsorbents, activated carbon (AC) impregnated with carbon moieties, has the ability to form a complex with different molecules, and this ability can vary [19].

Mestre et al. [23] reported that by activating a certain procedure, particles with tiny pores, a large surface area (ranging from 950–2000 m^2/g), a well-developed pore structure, and active surface properties are obtained. These characteristics enable efficient adsorption of smaller organic compounds, demonstrating that the adsorbent derived from biomass waste exhibits greater selectivity in eliminating ibuprofen. Terzyk et al. [24,25] found that modifying the surface with H_2SO_4 led to higher efficiency in drug removal compared to using HNO_3 and NH_3. Macías-García et al. [26] conducted research to examine the effects of varying concentrations of H_3PO_4 (30–85%) on the chemical modification and adsorption capacity of AC that was prepared from kenaf. But $ZnCl_2$, NaOH, and KOH are commonly favored as activation agents due to the fact that the resultant materials typically exhibit a distinct porous structure and high surface area, and they yield good production results [27].

The Argan tree covers of 871.210 ha of woodland in the fertile regions of the Souss Valley, nearly 17% of the Moroccan forest area [28]. In the past, the extraction of Argan Oil was primarily conducted by Moroccan women who utilized stone mill pressing.

The traditional extraction method often took place under unsanitary conditions. Fortunately, the introduction of mechanical cold-pressing has resolved this issue. This modern technique minimizes the need for manual labor while enhancing the quality of Argan Oil and regenerating higher quantities of byproducts including Argan paste cake [29].

Traditionally, the Argan paste cake was considered a waste material and was often discarded or used as animal feed. However, recent developments have highlighted the potential value of this byproduct. Researchers and manufacturers have started exploring alternative uses for Argan paste cake, transforming it from a waste material into a valuable resource [30]; in this context, the objective of this study is to explore the potential of Argan paste cake as unprocessed material for producing activated carbon through the use of KOH as an activation agent. Additionally, this research assesses its effectiveness in eliminating paracetamol for the first time. To achieve this goal, activated carbon samples were prepared from Argan paste cake to achieve best adsorption performance capacity, and a comparison study was conducted between the prepared samples and commercial GAC (granular activated carbon) prepared from coconut waste. Many studies have been carried out using this commercial activated carbon like a study of the application of enzyme-immobilized activated carbon for the removal of emerging pollutants from water [31] to remove micropollutants from municipal wastewater [32]. Following the adsorption of paracetamol in distilled water, the adsorbent exhibiting the most favorable outcomes for paracetamol elimination was chosen for a comprehensive analysis side by side with the commercial activated carbon (GAC), to measure the influence of the mass of adsorbent, pH, contact time, temperature, and adsorbent activation conditions on paracetamol removal from aqueous solution.

2. Materials and Methods

2.1. Materials and Pre-Treatment

The carbon precursor employed in this study was obtained from Argan paste cake sourced from a small village named Tizgui, located near the city of Tafraout in southwestern Morocco. To ensure its purity, the raw material underwent a thorough washing process using distilled water. Subsequently, it was dried for 24 h at 110 °C in an oven to remove any excess moisture. Once completely dried, the material was carefully crushed and stored in airtight plastic containers for future use. All the chemicals utilized in this research were of analytical grade and procured from Sigma-Aldrich located at Madrid, Spain.

2.1.1. Activation and Carbonization

The prepared raw material was carbonized under nitrogen flow of 300 mL/min for 1 h at 300 °C after cooling down. The resulting biochar was crushed and mixed with KOH (1:1) ratio for activation under nitrogen flow of 300 mL/min for 1 h with 800 °C; after cooling down, the activated carbon was then crushed and neutralized used HCL 1 M until achieving neutral pH. Then, it was subsequently washed using distilled water to eliminate the excess KOH and ash. The activated carbon was preserved in an oven for 24 h at 90 °C and to prevent moisture it was kept in a desiccator.

2.1.2. Granular Activated Carbons (GACs)

This study examined a commercially accessible granular activated carbon (GAC) sample, specifically activated carbon 12 × 40 mesh, supplied by AquaSorb®CT [33] to evaluate its performance. The granular activated carbon (GAC) sample used for this study possesses a substantial surface area around 1100 m^2/g and is characterized by particle sizes ranging from 0.5 to 1.7 mm; more properties of the utilized GAC are presented in (Table 1).

Table 1. Textural properties of APC-300-800 and GAC.

Samples	S_{BET} (m^2/g)	V_{N2} (cm^3/g)	V_{CO2} (cm^3/g)	V_{meso} (cm^3/g)	V_T (cm^3/g)	Yield
APC-300-800	1937	0.97	0.89	0.12	1.09	24.53%
GAC	1068	0.49	0.41	0.03	0.51	-

2.2. Characterization

To determine the optimal operating parameters for the preparation of activated carbon, various analytical instruments were employed. The surface morphology and structure were examined using a high-resolution field-emission scanning electron microscope (UHR FE-SEM Hitachi SU8020) with cold emission. Specific surface area and porosity analysis were carried out by calculating the N_2 adsorption/desorption isotherms at −196 °C and CO_2 adsorption at 0 °C, utilizing a volumetric QUADRASORB evoTM apparatus. The structural changes in the crystals of the carbonaceous materials were evaluated using X-ray diffraction (XRD) with Cu Kα radiation (λ = 1.54056 Å) on a PANalytical Empyrean X-ray diffractometer.

2.3. Adsorption Experiments

The adsorption properties of activated carbon, specifically prepared for the removal of paracetamol, were investigated through experimental studies using a Jasco V-630 UV-Vis Spectrophotometer. Measurements were taken at a wavelength of 245 nm. Stock solutions of paracetamol were prepared using distilled water, with a concentration of 1000 mg/L, by dissolving 1000 mg of paracetamol in 1 L of distilled water. Required concentrations for the experiments were obtained by diluting the stock solution accordingly. Batch adsorption experiments were conducted in a series of stoppered 100 mL Erlenmeyer flasks to evaluate the impact of various parameters on the removal of paracetamol using the prepared activated carbon. The important parameters examined included adsorbent

dose, solution pH, contact time, initial concentration, and temperature. The experimental conditions were set as follows: 30 mL of paracetamol solution, 10 mg of activated carbon, initial paracetamol concentration of 20 mg/L, natural pH of 5.8, stirring speed of 500 rpm, contact time of 60 min, and room temperature. Adjustments to the pH value were made using 0.1 M NaOH or HCl solution. To quantify the adsorption process, the amount of paracetamol adsorbed at equilibrium (q_e) was determined in mg/g, and the corresponding adsorption yield (%) was calculated using the following Equations (1) and (2) [34]:

$$q_e = \frac{(C_0 - C_e) \times V}{m}, \quad (1)$$

$$R(\%) = \frac{(C_0 - C_e)}{C_0} \times 100, \quad (2)$$

C_0 represents the initial paracetamol concentration in mg/L, C_e represents the concentration of paracetamol at equilibrium in mg/L, V represents the volume of the solution in liters, and m_{CA} represents the mass of the adsorbent in grams.

3. Results

3.1. Characterization of Materials

3.1.1. Textural Properties of APC-300-800

Many samples were studied in the preparation stage to achieve the best optimized sample to carry out the rest of this study. APC-300-800 has the best specific surface area reaching 1937 m^2/g with only a KOH/Biomass ratio of 1/1, micropore size of 0.97 cm^3/g, and total pore volume size of 1.09 cm^3/g. These details are illustrated in (Table 1). The N_2 adsorption desorption isotherm is type I and IV, which indicates that the sample is micro-mesoporous, according to the IUPAC classification [35].

The BET results (Figure 1) of the prepared sample, indicate a vast surface area available for adsorption per gram of activated carbon. A higher specific surface area suggests enhanced adsorption capacity and a greater number of active sites. The KOH/Biomass ratio of 1/1 represents the proportion of potassium hydroxide (KOH) used in relation to the Argan paste cake biomass during the activation process. This ratio significantly influences the development of porosity and, consequently, the resulting surface area of the activated carbon. The activated carbon exhibits a micropore size of 0.97 cm^3/g. The micropores are characterized by their small dimensions, typically less than 2 nm. The substantial micropore volume suggests a considerable capacity for adsorption of small molecules, owing to the extensive surface area and narrow pore size distribution. The total pore volume of the activated carbon is measured at 1.09 cm^3/g. This value represents the collective volume of all types of pores within the activated carbon per gram. The presence of a significant total pore volume implies an extensive pore network, encompassing both micropores and larger mesopores or macropores. It indicates the potential for efficient adsorption of diverse substances.

3.1.2. XRD Analysis

The XRD pattern (Figure 2) shows distinctive diffraction peaks at $2\theta = 25.56^\circ$ and $2\theta = 43.16^\circ$, which are assigned to the (002) and (100) graphitic planes [36], respectively. The strongest diffraction peak at around $2\theta = 25^\circ$ corresponds to the (002) graphitic plane. This peak indicates the ordered arrangement of carbon atoms within the activated carbon structure. The (002) plane represents the stacking of graphene layers, and its presence suggests the presence of well-developed graphitic structures in the activated carbon.

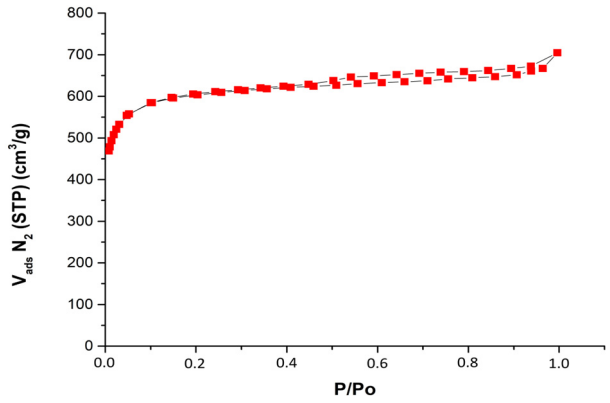

Figure 1. N_2 adsorption and desorption isotherm for APC-300-800 sample.

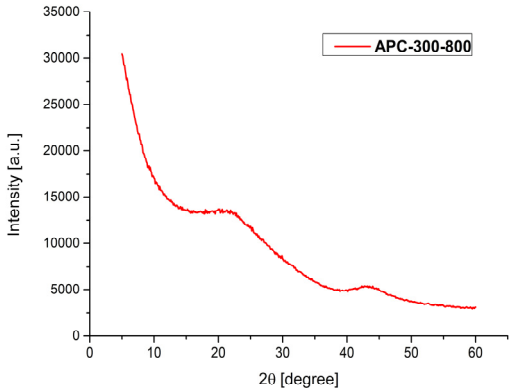

Figure 2. XRD pattern of the activated carbon sample APC-300-800.

The small diffraction peak at 2θ = 43.16° is assigned to the (100) graphitic plane. This peak indicates the presence of additional graphitic structures in the activated carbon. The (100) plane is related to the spacing between the carbon layers within the graphite-like structures present in the activated carbon. The presence of distinct diffraction peaks assigned to graphitic planes suggests that the activated carbon derived from Argan paste cake possesses a well-ordered graphitic structure. These graphitic planes contribute to the formation of a high specific surface area and can enhance the adsorption properties of the activated carbon.

3.1.3. SEM Images

The morphology of the activated carbon derived from Argan paste cake is shown in Figure 3b, representing the image after activation. Figure 3a is the image of the raw material with the effect of both activation and carbonization observable on the morphology of the carbon matrix, with creation of new pore sites with heterogeneous distribution caused by two-step pyrolysis. On the other hand, SEM images show a distribution of different pore sizes and shapes.

3.2. Adsorption Process

3.2.1. Influence of Adsorbent Dosage

The influence of adsorbent dosage on the adsorption of paracetamol was investigated to determine the optimal amount of activated carbon (APC-300-800/GAC) required for effective removal. The study explored a dosage range from 10 mg to 50 mg. The results, presented in (Figure 4), indicate that increasing the adsorbent dosage led to a corresponding increase in the percentage of paracetamol removal. Specifically, the percentage of paracetamol removal rose from 79.23% to 84.83% and from 13.89% to 84.35% when the dosage of APC-300-800/GAC increased from 10 mg to 50 mg, respectively. This observation can be

attributed to an augmented availability of adsorption sites and an enhanced contact area between the solid and liquid phases, facilitating greater paracetamol adsorption [37]. For the subsequent adsorption experiments, a dosage of 30 mg of APC-300-800 was selected as the optimal amount.

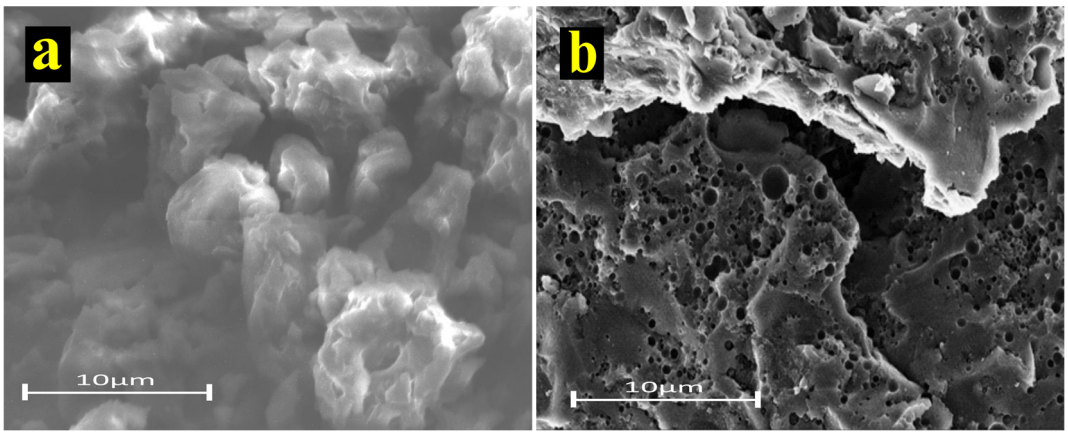

Figure 3. SEM images of the raw material (**a**) and APC-300-800 (**b**).

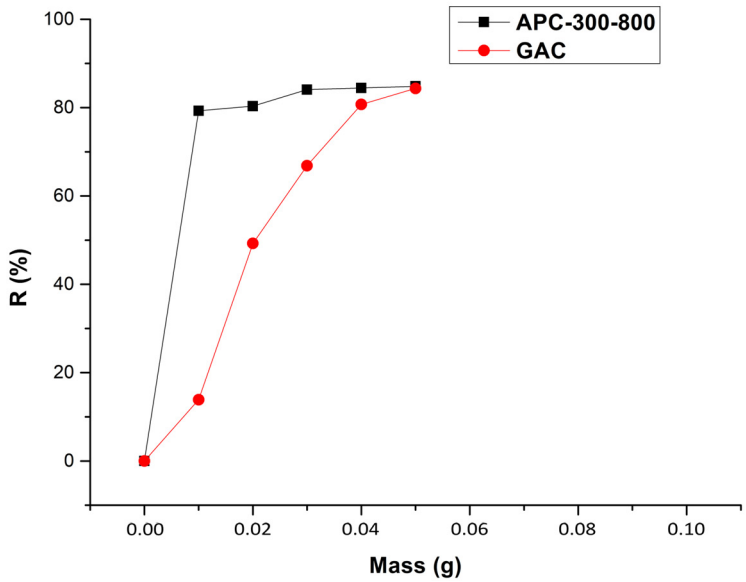

Figure 4. The impact of adsorbent dose on the adsorption of paracetamol using activated carbon APC-300-800/GAC.

3.2.2. Influence of Contact Time

The rate of adsorption is a critical parameter in understanding the kinetics of the adsorption process. To determine the time required to reach adsorption equilibrium for paracetamol, experiments were conducted using APC-300-800/GAC powder in Erlenmeyer flasks. The flasks contained a paracetamol solution of 30 mL with an initial temperature of 293 K, an initial pH of 6.6, and an initial concentration of 20 mg/L. Figure 5 illustrates the variation of the adsorbed quantity over time. As observed, the adsorbed amount of paracetamol increased with increasing contact time until reaching the equilibrium phase. Within the first 5 min, APC-300-800 demonstrated rapid adsorption, eliminating approximately 62.74% of paracetamol. After approximately 15 min, it reached a significant removal rate. However, it continued to adsorb at a much slower rate, ultimately reaching equilibrium after 120 min. On the other hand, it was observed that GAC exhibited slower adsorption, removing approximately 24.31% of paracetamol in 90 min, with the maximum removal of

56.62% achieved after 180 min. These outcomes can be attributed to the initial openness and accessibility of the adsorption sites, enabling efficient interaction with paracetamol molecules. Additionally, the rapid and substantial adsorption of paracetamol by APC-300-800 can be attributed to its larger surface area, its higher porosity, and the use of KOH-modified groups as catalysts during activation. More details for these models are provided in Table 2.

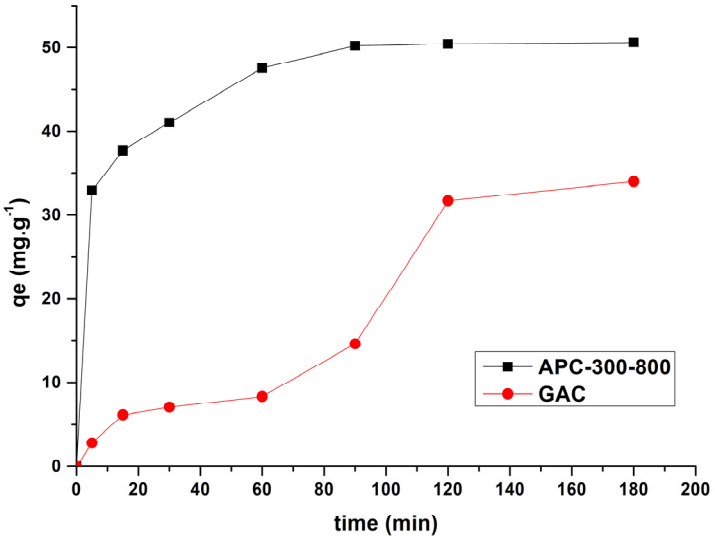

Figure 5. Influence of contact time on paracetamol removal by activated carbon APC-300-800/GAC.

Table 2. Kinetic parameters for the adsorption of paracetamol on APC-300-800/GAC.

		Biomass	
Models	**Parameters**	**APC-300-800**	**GAC**
Pseudo-first-order	q_e (mg/g)	38.2139	48.6620
	K_1 (1/min)	0.0467	0.0189
	R^2	0.955	0.7277
Pseudo-second-order	q_e (mg/g)	52.631	66.666
	K_2 (g/mg·min)	3.567×10^{-3}	6.741×10^{-5}
	R^2	0.9992	0.237
Elovich	α (mg/g·min)	8.1545	0.677
	β (g/mg)	0.3308	0.5100
	R^2	0.8907	0.6511
Intraparticle diffusion	K_{int} (g/mg·$min^{(1/2)}$)	1.04	0.8633
	C	6.02	1.3801
	R^2	0.7022	0.8407

3.2.3. Influence of pH

Numerous studies have highlighted the significance of pH as a crucial factor in the adsorption process. pH plays a pivotal role in determining the efficiency and effectiveness of adsorption mechanisms. By manipulating the pH of a solution, researchers have observed notable variations in the adsorption behavior and performance of different adsorbents. These findings collectively emphasize the importance of considering pH as a fundamental parameter when investigating and optimizing adsorption processes [38]. The influence of pH on the adsorption of paracetamol was thoroughly investigated. The pH of the solution was systematically varied from 2 to 11 at room temperature, using initial concentrations

of 20 mg/L. Precise pH adjustments were made by adding either 0.1 M HCl or NaOH solution to ensure accurate control. The obtained results, depicted in Figure 6, highlight the pivotal role of pH in the adsorption process. It is evident from the findings that the pH of the solution significantly affects the adsorption behavior of paracetamol. For APC-300-800, the percentage of paracetamol adsorbed gradually decreases as the pH increases, reaching a minimum value of 42.28%. Conversely, for GAC, the percentage of paracetamol adsorbed initially increases from pH 2 to 5, but then declines to a minimum of 2.70% at pH 11. These results indicate that higher pH levels lead to a reduction in the amount of paracetamol adsorbed. The optimal pH value for efficient adsorption using APC-300-800 is 2, while GAC demonstrates the highest adsorption capacity at a pH of 5. These findings underscore the importance of considering pH as a critical parameter in the adsorption process, as it directly influences the efficacy of paracetamol removal using different adsorbents.

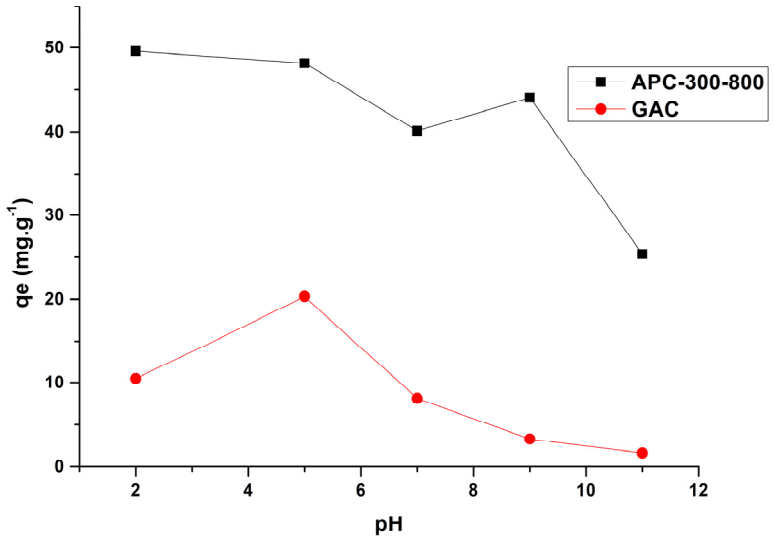

Figure 6. Influence of pH on paracetamol removal by activated carbon APC-300-800/GAC.

3.2.4. Influence of Concentration

The impact of initial paracetamol concentration on the adsorption process was thoroughly investigated, as illustrated in Figure 7. Different concentration ranges, ranging from 10 mg/L to 100 mg/L, were examined while keeping the time and temperature constant. The findings revealed a clear relationship between the concentration of paracetamol and its adsorption efficiency and capacity. It was observed that as the initial paracetamol concentration increased, the adsorption efficiency and capacity decreased. This phenomenon can be attributed to the limited availability of active adsorption sites on the surface of the adsorbent. At lower concentrations, there are sufficient vacant sites for paracetamol molecules to occupy, leading to higher removal efficiency. However, as the concentration in the solution increases, the active sites become occupied, resulting in reduced removal of paracetamol from the solution. Interestingly, both the removal efficiency and adsorption capacity exhibited similar characteristics. Initially, there was a rapid and significant increase in both parameters for both adsorbents. This behavior can be attributed to the abundance of vacant sites on the carbon surface during the initial stages of adsorption. However, as the process continued, the remaining vacant sites were influenced by repulsive forces between the molecules on the carbon surface. These findings highlight the intricate relationship between initial paracetamol concentration and its adsorption behavior [39].

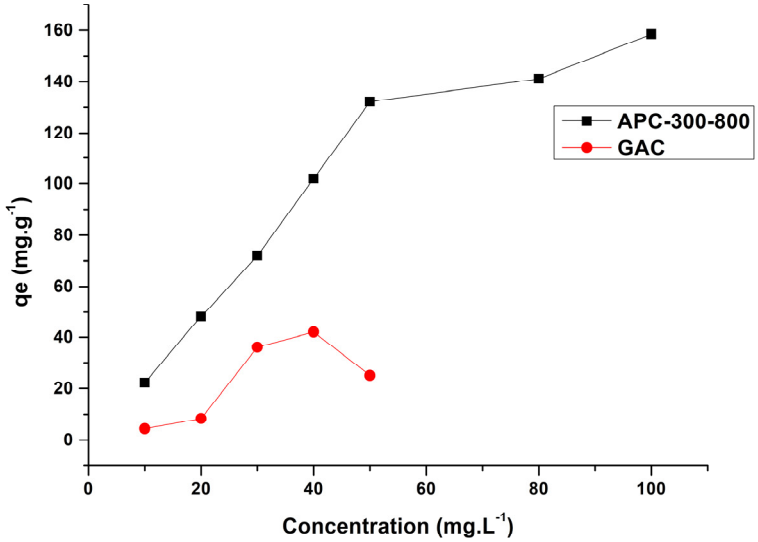

Figure 7. Influence of initial concentration on paracetamol removal by activated carbon APC-300-800/GAC.

Hence, these findings provide further evidence that enhancing the diffusion of paracetamol molecules can be achieved by facilitating improved transport pathways, primarily through the utilization of a large surface area that offers abundant adsorption sites. These results underscore the importance of optimizing the adsorbent's structural characteristics to enhance the efficiency of paracetamol adsorption.

3.3. Kinetic Study

To comprehensively understand the adsorption processes of the paracetamol molecule, the experimental data obtained were subjected to modeling using various kinetic models, including the pseudo-first-order [40], pseudo-second-order [41], Elovich [42], and intra-particle kinetic models [40]. The corresponding equations for these models are presented below:

$$\mathrm{Ln}(q_e - q_t) = \mathrm{Ln}q_e - K_1 t \quad (3)$$

$$\frac{t}{q_t} = \frac{1}{K_2 \cdot {q_e}^2} + \frac{t}{q_e}, \quad (4)$$

$$qt = \frac{1}{\beta}\ln(\alpha\beta) + \frac{1}{\beta}\ln\ t, \quad (5)$$

$$qt = K_{int}\sqrt{t} + C, \quad (6)$$

q_e (mg/g): Adsorption amount of paracetamol at equilibrium;
q_t (mg/g): Amount of paracetamol adsorbed onto the solid phase at time t;
k_1 (1/min): Pseudo-first-order rate constant;
k_2 (g/mg·min): Pseudo-second-order rate constant;
α (mg/g·min): Initial adsorption coefficient;
β (g/mg): Desorption coefficient;
K_{int} (g/mg·min$^{(1/2)}$): Rate constant of the intra-particle diffusion model;
C: Constant.

The kinetics models were evaluated and presented in Figure 8, while the parameter values obtained for each model are listed in Table 2. To determine the best-fitting kinetic model, the fitting parameters were compared, with a focus on achieving high coefficient of determination values ($R^2 > 0.9992$). For the adsorption of paracetamol by APC-300-800, the pseudo-second-order model exhibited a better fit to the experimental data compared to the pseudo-first-order and Elovich models. This suggests that the rate-determining step

in the adsorption process is likely the movement of the adsorbate mass from the solution to the surface of the adsorbent [43]. Conversely, for the adsorption of paracetamol by GAC, the pseudo-first-order model provided a better fit, with an R^2 value exceeding 0.7277. Additionally, the pseudo-second-order model has been widely recognized as a suitable model for describing paracetamol adsorption on various activated carbon adsorbents, as reported in previous studies [44]. The data obtained was consistent with the experimental data obtained in Figure 8.

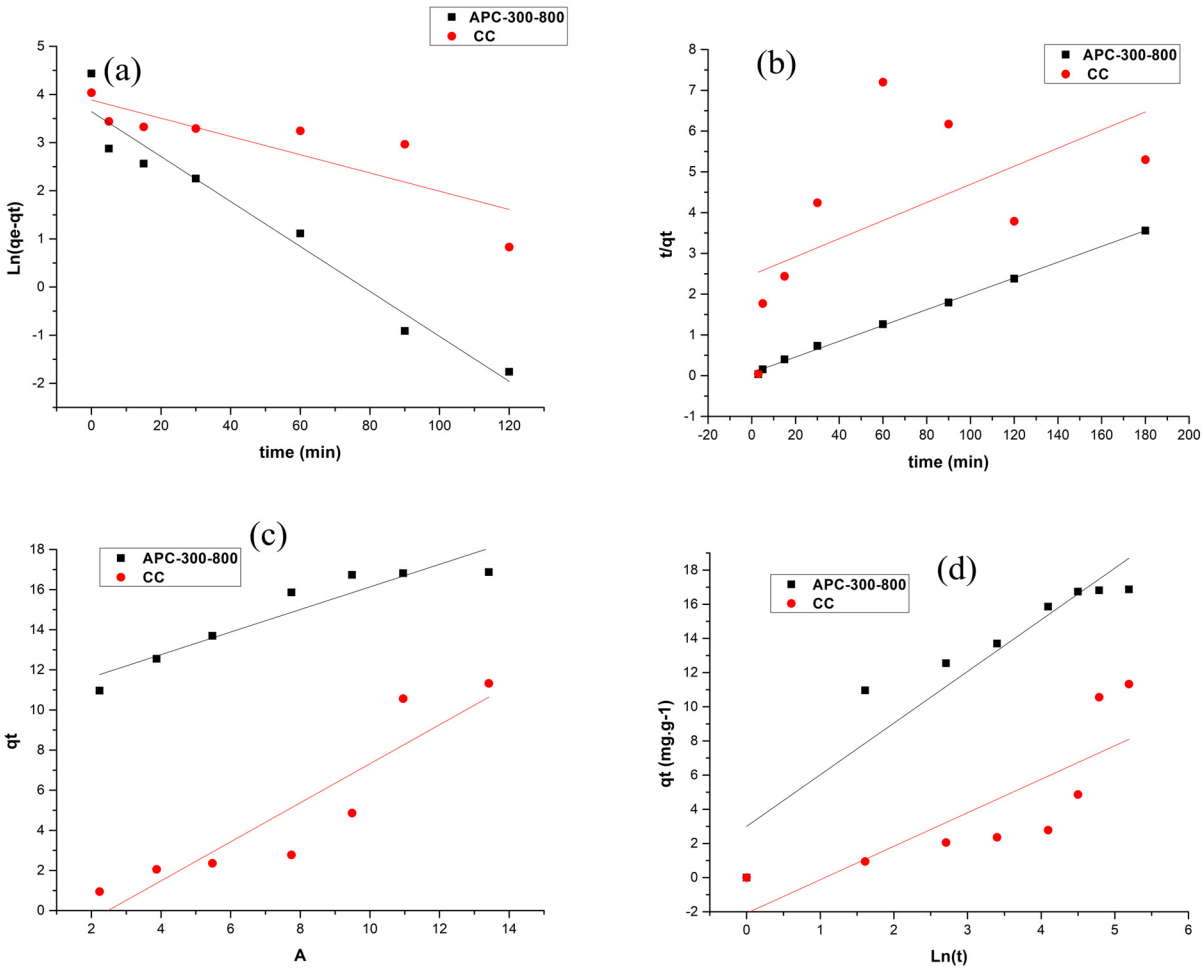

Figure 8. Linear plots of pseudo-first-order (**a**), pseudo-second-order (**b**), intraparticle (**c**), Elovich, and (**d**) kinetic models, respectively.

3.4. Isotherm Studies

Adsorption isotherms are the key word for better understanding of the relationship in the adsorption phenomena of adsorbate/adsorbent; in modeling those isotherms we can predict the performance of the adsorption system, capacity of adsorbent, mechanism of adsorption, and adsorption performance evaluation. All these parameters are provided using the models. In this study Langmuir [45], Freundlich [46], Temkin [47], and Dubinin–Radushkevich [48] are the models used to fit the experimental results of both our activated carbon APC-300-800 and granular activated carbon (GAC) in adsorption tests of paracetamol molecules. The following are the models of Equations (7)–(10), respectively:

$$\frac{C_e}{Q_e} = \frac{C_e}{Q_{max}} + \frac{1}{K_L \cdot Q_{max}}, \quad (7)$$

where Q_e is the adsorbed amount in (mg/g), Q_{max} represents maximal adsorbed amount in (mg/g), and C_e and K_L are the equilibrium concentration in (mg/L) and Langmuir adsorption constant, respectively.

$$\mathrm{Ln}(Q_e) = \ln\,(\mathrm{KF}) + \frac{1}{n}\ln(C_e), \tag{8}$$

where KF represents the Freundlich constant, C_e is the equilibrium concentration in (mg/L), Q_e is the amount in (mg/g) of absorbed molecules, and n is linearity value of adsorbate/adsorption solution process.

$$Q_e = \frac{RT}{b}\ln(C_e) + \frac{RT}{b}\ln(K_T), \tag{9}$$

where R_T/b represent heating constant of the adsorption, K_T is the constant of binding equilibrium, and T is the temperature.

$$\mathrm{Ln}\,(Q_e) = \mathrm{Ln}\,(Q_s) - K_{ad}\,\epsilon^2, \tag{10}$$

where K_{ad} represents the Dubinin–Radushkevich constant, Q_S represents theoretical isotherms' saturation capacity, and ϵ in (J/mol) refers to the Polanyi potential.

3.4.1. Plotting and Analysis of Langmuir Model

Langmuir model adsorption parameters were obtained using Equation (7). All adsorption parameters are determined in Table 3. The plotting graph of the Langmuir isotherm is illustrated in Figure 9a. Both adsorption precursors have a small K_L value; therefore, we understand a weak absorbent/adsorbate interaction due to the active site adsorbing only one molecule. The maximum adsorption capacity is 344.827 mg/g for APC-300-800 and 13.106 mg/g for GAC; the R_L values obtained were between 0 and 1 and show that the adsorption of paracetamol onto the APC-300-800 and GAC was favorable.

Table 3. Langmuir isotherm parameters.

Precursor	Q_{max} (mg·g^{-1})	K_L (L·mg^{-1})	R_L	R^2	Note
APC-300-800	344.827	0.0275	0.78	0.8497	$0 < R_L < 1$ adsorption is favorable, $R^2 > 0.70$ monolayer adsorption
GAC	13.1061	0.0291	0.77	0.868	$0 < R_L < 1$ adsorption is favorable, $R^2 > 0.70$ monolayer adsorption

Plotting graphs show that GAC and APC-300-800 have a relatively high correlation value ($R^2 > 0.70$); we can then say that they are well presented using the Langmuir isotherm.

3.4.2. Plotting and Analysis of Freundlich Isotherm

All Freundlich parameters were obtained using Equation (8); C_e and Q_e values were transformed to ln C_e and ln Q_e, which are used to plot data illustrated in Table 4. The data graph results are illustrated in Figure 9b. The adsorption parameters are also determined using results of data fitting in Table 4. The Freundlich isotherm fits better for the APC-300-800 adsorption system than for GAC, which can be confirmed by R^2 surpassing 0.70 with physical interactions.

Table 4. Freundlich isotherm parameters.

Precursors	1/*n*	R^2	Note
APC-300-800	0.5065	0.6122	$0 < 1/n < 1$ means favorable adsorption process $n < 1$, adsorption process with physical interaction $R^2 > 0.70$, multilayer adsorption
GAC	1.2508	0.5491	$1/n > 1$, cooperative adsorption $n < 1$, chemical interaction between adsorbate molecules $R^2 < 0.70$, monolayer adsorption

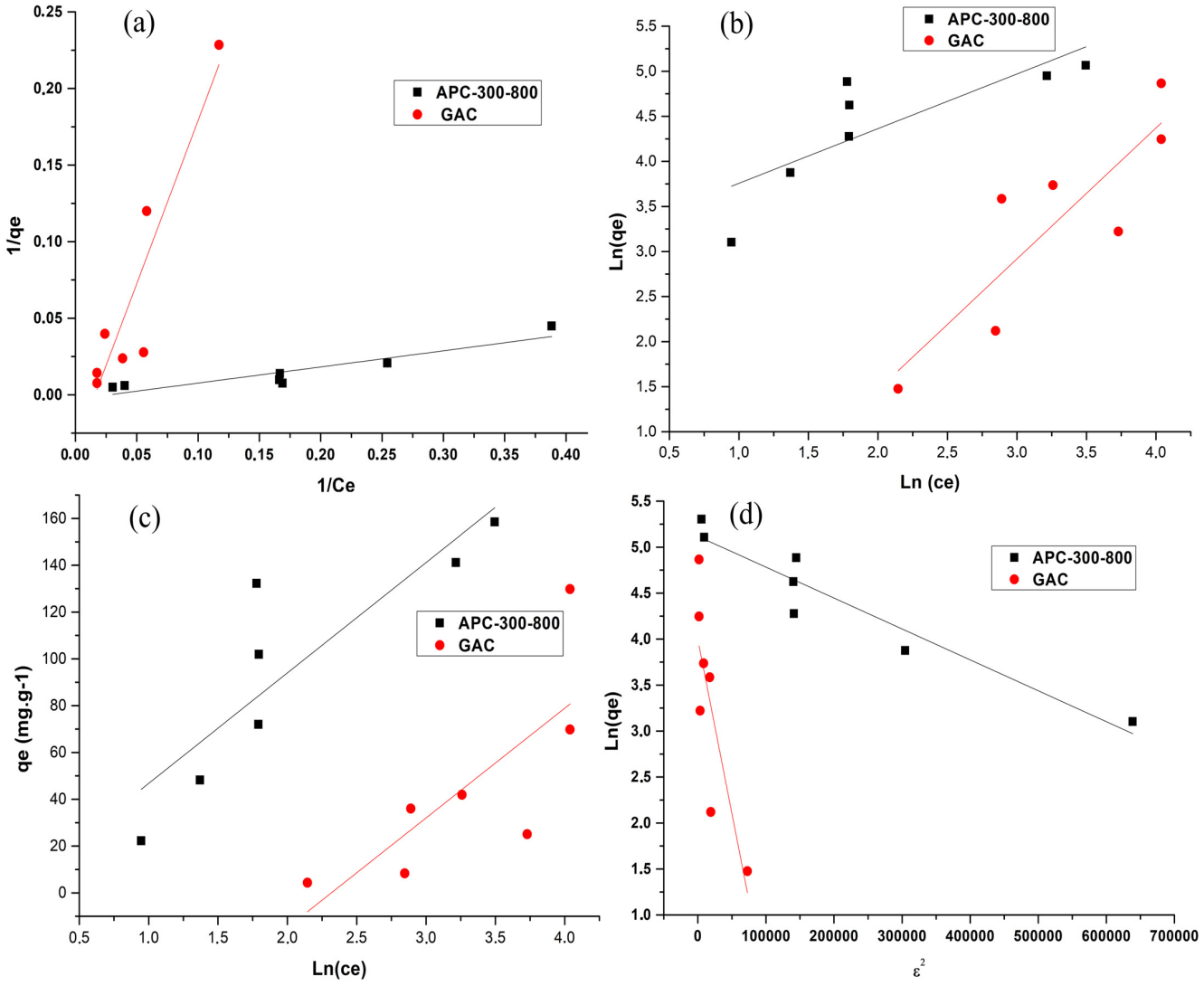

Figure 9. Isotherm plots of Langmuir (**a**), Freundlich (**b**), Temkin (**c**), and Dubinin–Radushkevich (**d**).

3.4.3. Plotting and Analysis of Temkin Isotherm

Temkin parameters were revealed from ln C_e and Q_e data plotting, as shown in Figure 9c. From Equation (9), the obtained parameters are R^2, b, and K_T. Table 5 gathers all the results of the used precursors APC-300-800 and GAC.

Table 5. Temkin isotherm parameters.

Precursor	K_T (L·mg^{-1})	B_T (J·mol^{-1})	R^2	Note
APC-300-800	40.449	60.116	0.7342	B_T < 8 kJ/mol Physical interaction between adsorbate molecules R^2 > 0.70, adsorbate/adsorbent surface uniform distribution
GAC	0.0985	157.439	0.5804	B_T < 8 kJ/mol Physical interaction between adsorbate molecules R^2 < 0.70, no adsorbate/adsorbent surface uniform distribution

3.4.4. Plotting and Analysis of Dubinin–Radushkevich

To draw and to obtain Dubinin–Radushkevich isotherm and adsorption parameters illustrated in Table 6, Equation (10) was used. Q_e was transformed to lnQ_e and calculated $\mathcal{E}^2$ to plot the data, which is represented in Figure 9d, revealing that the APC-300-800 adsorption system has a correlation coefficient higher than (R^2 > 0.70) showing the highest R^2 value comparing to all other models, so it is considered according to Dubinin–Radushkevich to have micropore size structure, while GAC represents a correlation coefficient lower than (R^2 > 0.70).

Table 6. Dubinin–Radushkevich isotherm parameters.

Precursor	q_m (mg·g^{-1})	E (kJ·mol^{-1})	K_{ad}	R^2	Note
APC-300-800	166.967	385,761	3.10–6	0.89665	R^2 > 0.70, micropore size exists in adsorbent surface
GAC	54.266	114,992	3.10–5	0.58757	R^2 < 0.70, no micropore size exists in adsorbent surface

3.5. Thermodynamic Studies

To examine the absorption characteristics of paracetamol on APC-300-800/GAC, we employed the thermodynamic properties, namely the change in free energy (ΔG°), enthalpy (ΔH°), and entropy (ΔS°), to elucidate the adsorption behavior. The values for these parameters were determined using the subsequent equations:

$$\Delta G^\circ = -\,RTLn(Kd), \text{ and } \Delta G^\circ = \Delta H^\circ - T\Delta S^\circ, \tag{11}$$

$$Ln(Kd) = \frac{\Delta S^\circ}{R} - \frac{\Delta H^\circ}{RT}, \tag{12}$$

$$Kd = \frac{Q_e}{C_e}, \tag{13}$$

where T is the kelvin temperature (K), K_d is the distribution constant in (L·g^{-1}), and R is the gas constant (8.314 J·mol·K^{-1}).

Table 7 shows the thermodynamic parameters of paracetamol on APC-300-800/GAC. The plot of the ln(k_d) curve as a function of 1/t results in a straight line with a slope equal to—ΔH°/R and an origin ordinate equal to ΔS°/R, as illustrated in Figure 10. The negative value of ΔG° indicates that the adsorption of paracetamol on APC-300-800/GAC was spontaneous. Additionally, the positive ΔH° values suggest that the sorption of paracetamol on APC-300-800/GAC was endothermic, and the adsorption capacity increased with temperature. The positive ΔS° reflects the increased randomness of the system due to the strong binding of the paracetamol molecule to APC-300-800/GAC during the adsorption process. Moreover, the adsorption process was attributed to physical adsorption when

$2.1 < \Delta H^\circ < 20.9$ Kj.mol^{-1}, and the acting force may be Van der Waals force or electrostatic interaction. On the other hand, when $20.9 < \Delta H^\circ < 418.4$ Kj.mol^{-1}, the adsorption process was attributed to chemical adsorption [49]. The value for the GAC adsorbent was 96.126 kJ/mol. Therefore, the primary adsorption mechanism of paracetamol on APC-300-800 was physisorption, while for GAC, it was chemisorption.

Table 7. Thermodynamics parameters for the adsorption of paracetamol on APC-300-800/CC.

Adsorbents	ΔG° (kJ·mol^{-1})			ΔH° (kJ·mol^{-1})	ΔS° (J·mol^{-1}·K^{-1})
	298 (K)	318 (K)	338 (K)		
APC-300-800	−151.74	−556.78	−575.19	10.152	54.3270
GAC	−5.454	−12.271	−19.089	96.126	340.874

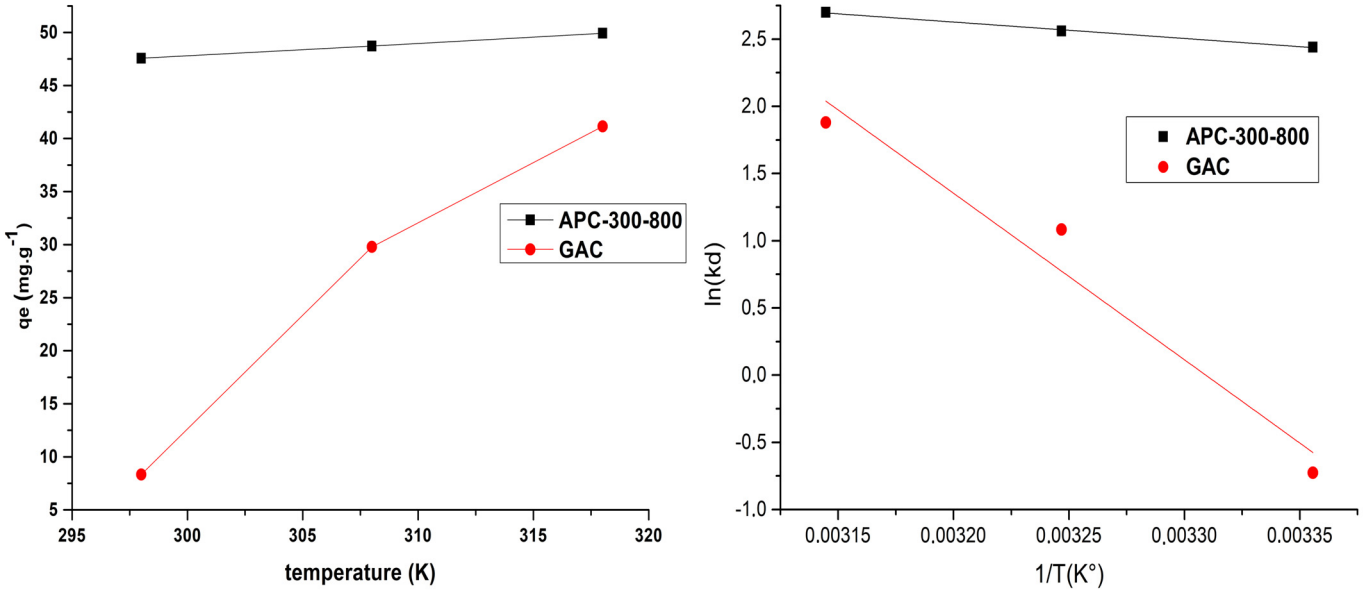

Figure 10. Temperature impact on the adsorption of paracetamol by APC-300-800/GAC.

3.6. Regeneration Studies

The ability of the adsorbents to be reused is a major property that determines whether the process is economically applicable. The regeneration cycles, in regards to economic evaluation, were performed to further evaluate the application of APC-300-800 as an adsorbent for the removal of pharmaceutical compounds. The regeneration process was performed with an initial paracetamol concentration of 20 mg·L^{-1} and under optimized conditions (pH = 2, contact time of 60 min, and an adsorbent amount of 10 mg). The result is presented in Figure 11, in which it is clearly noted that the percentage of paracetamol removed decreases from 96.81% to 95.93%. By performing five adsorption–desorption cycles, the fact that paracetamol loaded on APC-300-800 adsorbent is reusable was confirmed. In all five cycles, paracetamol was adsorbed. These results revealed that APC-300-800 has the potential to be reused several times and could be an efficient, economical, and eco-friendly adsorbent.

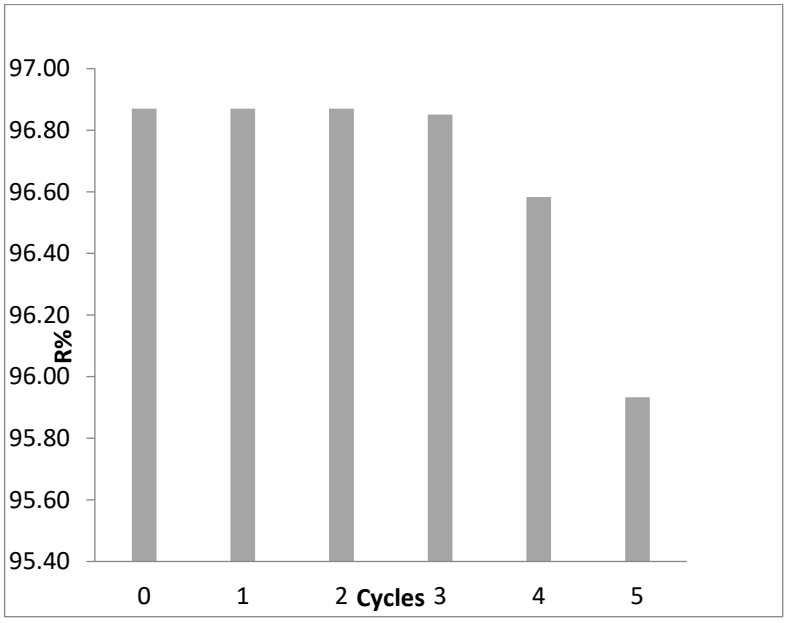

Figure 11. Number of cycles to test reusability of APC-300-800.

4. Conclusions

In conclusion, this study successfully prepared and characterized activated carbon derived from Argan paste cake through carbonization and activation processes. The obtained sample, APC-300-800, exhibited a high surface area of 1937 m^2/g, as determined using BET analysis. The comparison between APC-300-800 and a commercially available granular activated carbon (GAC) highlighted the superior adsorption capacity of APC-300-800.

The adsorption tests demonstrated that the adsorption kinetics of paracetamol on APC-300-800 followed the second pseudo-order model, indicating a favorable adsorption rate. The Dubinin–Radushkevich isotherm model accurately described the adsorption behavior, with an R^2 value of 0.89665, further confirming the efficacy of APC-300-800 as an adsorbent for paracetamol.

Moreover, the Langmuir model revealed that APC-300-800 achieved a maximum adsorption capacity of 344.827 mg/g for paracetamol, showcasing its high adsorption performance. In contrast, GAC exhibited chemisorption behavior.

Thermodynamic studies indicated that the adsorption process on APC-300-800 was primarily governed by physisorption. This finding implies that APC-300-800 has the potential to be an efficient adsorbent for water treatment applications, where physisorption is often preferred due to its reversible and energy-efficient nature.

Overall, the results of this study demonstrate that APC-300-800, derived from Argan paste cake, possesses exceptional adsorption properties, outperforming the commercially available GAC. The high surface area, favorable adsorption kinetics, and significant adsorption capacity make APC-300-800 a promising candidate for various water treatment applications, contributing to the development of sustainable and effective adsorbents in environmental remediation efforts.

Author Contributions: Conceptualization, E.H.Y. and M.O.; methodology, E.H.Y.; software, E.K.C.; validation, M.S., M.O. and E.K.C.; formal analysis, M.O.; investigation, E.H.Y., F.C. and E.K.C.; resources, M.S., F.C. and E.K.C.; writing—original draft preparation, E.H.Y. and A.T.; writing—review and editing, E.H.Y. and E.K.C.; visualization, M.S.; supervision, M.S. and M.O.; project administration, M.S. All authors have read and agreed to the published version of the manuscript.

Funding: This research received no external funding.

Institutional Review Board Statement: Not applicable.

Informed Consent Statement: Not applicable.

Data Availability Statement: Not applicable.

Acknowledgments: The authors gratefully thank EL ADNANI IKRAM for the support and for use of the equipment.

Conflicts of Interest: The authors declare no conflict of interest.

References

1. Carvalho, I.T.; Santos, L. Antibiotics in the Aquatic Environments: A Review of the European Scenario. *Environ. Int.* **2016**, *94*, 736–757. [CrossRef] [PubMed]
2. Petrie, B.; Barden, R.; Kasprzyk-Hordern, B. A Review on Emerging Contaminants in Wastewaters and the Environment: Current Knowledge, Understudied Areas and Recommendations for Future Monitoring. *Water Res.* **2015**, *72*, 3–27. [CrossRef]
3. Żur, J.; Piński, A.; Marchlewicz, A.; Hupert-Kocurek, K.; Wojcieszyńska, D.; Guzik, U. Organic Micropollutants Paracetamol and Ibuprofen—Toxicity, Biodegradation, and Genetic Background of Their Utilization by Bacteria. *Environ. Sci. Pollut. Res.* **2018**, *25*, 21498–21524. [CrossRef] [PubMed]
4. Mostafa, E.M.A.; Tawfik, A.M.; Abd-Elrahman, K.M. Egyptian Perspectives on Potential Risk of Paracetamol/Acetaminophen-Induced Toxicities: Lessons Learnt during COVID-19 Pandemic. *Toxicol. Rep.* **2022**, *9*, 541–548. [CrossRef] [PubMed]
5. Essawy, A.E.; Alkhuriji, A.F.; Soffar, A.A. Paracetamol Overdose Induces Physiological and Pathological Aberrations in Rat Brain. *J. Appl. Pharm. Sci.* **2017**, *7*, 185–190. [CrossRef]
6. Tittarelli, R.; Pellegrini, M.; Scarpellini, M.G.; Marinelli, E.; Bruti, V.; Luca, N.M.D.; Busardò, F.P.; Zaami, S. Hepatotoxicity of Paracetamol and Related Fatalities. *Eur. Rev. Med Pharmacol. Sci.* **2017**, *21*, 95–101.
7. Yoon, E.; Babar, A.; Choudhary, M.; Kutner, M.; Pyrsopoulos, N. Acetaminophen-Induced Hepatotoxicity: A Comprehensive Update. *J. Clin. Transl. Hepatol.* **2016**, *4*, 131–142. [CrossRef]
8. Ortúzar, M.; Esterhuizen, M.; Olicón-Hernández, D.R.; González-López, J.; Aranda, E. Pharmaceutical Pollution in Aquatic Environments: A Concise Review of Environmental Impacts and Bioremediation Systems. *Front. Microbiol.* **2022**, *13*, 869332. [CrossRef]
9. Teh, C.Y.; Budiman, P.M.; Shak, K.P.Y.; Wu, T.Y. Recent Advancement of Coagulation–Flocculation and Its Application in Wastewater Treatment. *Ind. Eng. Chem. Res.* **2016**, *55*, 4363–4389. [CrossRef]
10. Wu, S.; Zhang, L.; Chen, J. Paracetamol in the Environment and Its Degradation by Microorganisms. *Appl. Microbiol. Biotechnol.* **2012**, *96*, 875–884. [CrossRef]
11. Gogate, P.R.; Pandit, A.B. A Review of Imperative Technologies for Wastewater Treatment I: Oxidation Technologies at Ambient Conditions. *Adv. Environ. Res.* **2004**, *8*, 501–551. [CrossRef]
12. Chen, R.; Chai, L.; Wang, Y.; Liu, H.; Shu, Y.; Zhao, J. Degradation of Organic Wastewater Containing Cu–EDTA by Fe–C Micro-Electrolysis. *Trans. Nonferrous Met. Soc. China* **2012**, *22*, 983–990. [CrossRef]
13. Rad, L.R.; Haririan, I.; Divsar, F. Comparison of Adsorption and Photo-Fenton Processes for Phenol and Paracetamol Removing from Aqueous Solutions: Single and Binary Systems. *Spectrochim. Acta Part A Mol. Biomol. Spectrosc.* **2015**, *136*, 423–428. [CrossRef] [PubMed]
14. Bhattacharya, A. Remediation of Pesticide-Polluted Waters Through Membranes. *Sep. Purif. Rev.* **2006**, *35*, 1–38. [CrossRef]
15. Soltani, R.D.C.; Miraftabi, Z.; Mahmoudi, M.; Jorfi, S.; Boczkaj, G.; Khataee, A. Stone Cutting Industry Waste-Supported Zinc Oxide Nanostructures for Ultrasonic Assisted Decomposition of an Anti-Inflammatory Non-Steroidal Pharmaceutical Compound. *Ultrason. Sonochemistry* **2019**, *58*, 104669. [CrossRef]
16. Mirzaee, R.; Darvishi Cheshmeh Soltani, R.; Khataee, A.; Boczkaj, G. Combination of Air-Dispersion Cathode with Sacrificial Iron Anode Generating $Fe^{2+}Fe^{3+}{}_2O_4$ Nanostructures to Degrade Paracetamol under Ultrasonic Irradiation. *J. Mol. Liq.* **2019**, *284*, 536–546. [CrossRef]
17. Norra, G.-F.; Radjenovic, J. Removal of Persistent Organic Contaminants from Wastewater Using a Hybrid Electrochemical-Granular Activated Carbon (GAC) System. *J. Hazard. Mater.* **2021**, *415*, 125557. [CrossRef]
18. Karimi-Maleh, H.; Karimi, F.; Fu, L.; Sanati, A.L.; Alizadeh, M.; Karaman, C.; Orooji, Y. Cyanazine Herbicide Monitoring as a Hazardous Substance by a DNA Nanostructure Biosensor. *J. Hazard. Mater.* **2022**, *423*, 127058. [CrossRef]
19. Ndoun, M.C.; Elliott, H.A.; Preisendanz, H.E.; Williams, C.F.; Knopf, A.; Watson, J.E. Adsorption of Pharmaceuticals from Aqueous Solutions Using Biochar Derived from Cotton Gin Waste and Guayule Bagasse. *Biochar* **2021**, *3*, 89–104. [CrossRef]
20. Serafin, J.; Ouzzine, M.; Cruz Junior, O.F.; Sreńscek-Nazzal, J. Preparation of Low-Cost Activated Carbons from Amazonian Nutshells for CO_2 Storage. *Biomass Bioenergy* **2021**, *144*, 105925. [CrossRef]
21. Sajid, M.; Bai, Y.; Liu, D.; Zhao, X. Organic Acid Catalyzed Production of Platform Chemical 5-Hydroxymethylfurfural from Fructose: Process Comparison and Evaluation Based on Kinetic Modeling. *Arab. J. Chem.* **2020**, *13*, 7430–7444. [CrossRef]
22. Bary, G.; Jamil, M.I.; Arslan, M.; Ghani, L.; Ahmed, W.; Ahmad, H.; Zaman, G.; Ayub, K.; Sajid, M.; Ahmad, R.; et al. Regio- and Stereoselective Functionalization of Alkenes with Emphasis on Mechanistic Insight and Sustainability Concerns. *J. Saudi Chem. Soc.* **2021**, *25*, 101260. [CrossRef]

23. Mestre, A.S.; Bexiga, A.S.; Proença, M.; Andrade, M.; Pinto, M.L.; Matos, I.; Fonseca, I.M.; Carvalho, A.P. Activated Carbons from Sisal Waste by Chemical Activation with K_2CO_3: Kinetics of Paracetamol and Ibuprofen Removal from Aqueous Solution. *Bioresour. Technol.* **2011**, *102*, 8253–8260. [CrossRef] [PubMed]
24. Terzyk, A.P. The Impact of Carbon Surface Composition on the Diffusion and Adsorption of Paracetamol at Different Temperatures and at Neutral PH. *J. Colloid Interface Sci.* **2000**, *230*, 219–222. [CrossRef] [PubMed]
25. Terzyk, A.P. Adsorption of Biologically Active Compounds from Aqueous Solutions on to Commercial Unmodified Activated Carbons: Part II. Temperature Dependence of Adsorption Kinetics of 4-Hydroxyacetanilide (Paracetamol) at Neutral PH. *Adsorpt. Sci. Technol.* **2000**, *18*, 477–508. [CrossRef]
26. Macías-García, A.; García-Sanz-Calcedo, J.; Carrasco-Amador, J.P.; Segura-Cruz, R. Adsorption of Paracetamol in Hospital Wastewater Through Activated Carbon Filters. *Sustainability* **2019**, *11*, 2672. [CrossRef]
27. Song, X.; Zhang, Y.; Chang, C. Novel Method for Preparing Activated Carbons with High Specific Surface Area from Rice Husk. *Ind. Eng. Chem. Res.* **2012**, *51*, 15075–15081. [CrossRef]
28. Aithammou, R.; Harrouni, C.; Aboudlou, L.; Hallouti, A.; Mlouk, M.; Elasbahani, A.; Daoud, S. Effect of Clones, Year of Harvest and Geographical Origin of Fruits on Quality and Chemical Composition of Argan Oil. *Food Chem.* **2019**, *297*, 124749. [CrossRef]
29. Mechqoq, H.; El Yaagoubi, M.; Momchilova, S.; Msanda, F.; El Aouad, N. Comparative Study on Yields and Quality Parameters of Argan Oils Extracted by Conventional and Green Extraction Techniques. *Grain Oil Sci. Technol.* **2021**, *4*, 125–130. [CrossRef]
30. González-Fernández, M.J.; Manzano-Agugliaro, F.; Zapata-Sierra, A.; Belarbi, E.H.; Guil-Guerrero, J.L. Green Argan Oil Extraction from Roasted and Unroasted Seeds by Using Various Polarity Solvents Allowed by the EU Legislation. *J. Clean. Prod.* **2020**, *276*, 123081. [CrossRef]
31. Al-sareji, O.J.; Meiczinger, M.; Somogyi, V.; Al-Juboori, R.A.; Grmasha, R.A.; Stenger-Kovács, C.; Jakab, M.; Hashim, K.S. Removal of Emerging Pollutants from Water Using Enzyme-Immobilized Activated Carbon from Coconut Shell. *J. Environ. Chem. Eng.* **2023**, *11*, 109803. [CrossRef]
32. Benstoem, F.; Nahrstedt, A.; Boehler, M.; Knopp, G.; Montag, D.; Siegrist, H.; Pinnekamp, J. Performance of Granular Activated Carbon to Remove Micropollutants from Municipal Wastewater—A Meta-Analysis of Pilot- and Large-Scale Studies. *Chemosphere* **2017**, *185*, 105–118. [CrossRef] [PubMed]
33. Jacobi Aquasorb Catalytic Granular Coconut Shell-Based Activated Carbon. Available online: https://www.aquascience.net/jacobi-aquasorb-catalytic-granular-coconut-shell-based-activated-carbon (accessed on 2 June 2023).
34. Mamane, O.S.; Zanguina, A.; Daou, I.; Natatou, I. Préparation et caractérisation de charbons actifs à base de coques de noyaux de Balanites Eagyptiaca et de Zizyphus Mauritiana. *J. Société Ouest-Afr. Chim.* **2016**, *41*, 59.
35. Rouquerol, J.; Avnir, D.; Fairbridge, C.W.; Everett, D.H.; Haynes, J.H.; Pernicone, N.; Ramsay, J.D.F.; Sing, K.S.W.; Unger, K.K. Recommendations for the Characterization of Porous Solids (Technical Report). *Pure Appl. Chem.* **1994**, *66*, 1739–1758. [CrossRef]
36. Yoshizawa, N.; Maruyama, K.; Yamada, Y.; Ishikawa, E.; Kobayashi, M.; Toda, Y.; Shiraishi, M. XRD Evaluation of KOH Activation Process and Influence of Coal Rankq. *Fuel* **2002**, *81*, 1717–1722. [CrossRef]
37. El Khomri, M.; El Messaoudi, N.; Dbik, A.; Bentahar, S.; Lacherai, A. Efficient Adsorbent Derived from Argania Spinosa for the Adsorption of Cationic Dye: Kinetics, Mechanism, Isotherm and Thermodynamic Study. *Surf. Interfaces* **2020**, *20*, 100601. [CrossRef]
38. Li, H.; Budarin, V.L.; Clark, J.H.; North, M.; Wu, X. Rapid and Efficient Adsorption of Methylene Blue Dye from Aqueous Solution by Hierarchically Porous, Activated Starbons®: Mechanism and Porosity Dependence. *J. Hazard. Mater.* **2022**, *436*, 129174. [CrossRef]
39. Rincón-Silva, N.G.; Moreno-Piraján, J.C.; Giraldo, L.G. Thermodynamic Study of Adsorption of Phenol, 4-Chlorophenol, and 4-Nitrophenol on Activated Carbon Obtained from Eucalyptus Seed. *J. Chem.* **2015**, *2015*, 569403. [CrossRef]
40. Edet, U.A.; Ifelebuegu, A.O. Kinetics, Isotherms, and Thermodynamic Modeling of the Adsorption of Phosphates from Model Wastewater Using Recycled Brick Waste. *Processes* **2020**, *8*, 665. [CrossRef]
41. Taiwo, A.F.; Chinyere, N.J. Sorption Characteristics for Multiple Adsorption of Heavy Metal Ions Using Activated Carbon from Nigerian Bamboo. *J. Mater. Sci. Chem. Eng.* **2016**, *4*, 39–48. [CrossRef]
42. Musah, M.; Azeh, Y.; Mathew, J.; Umar, M.; Abdulhamid, Z.; Muhammad, A. Adsorption Kinetics and Isotherm Models: A Review. *CaJoST* **2022**, *4*, 20–26. [CrossRef]
43. Spaltro, A.; Pila, M.N.; Colasurdo, D.D.; Noseda Grau, E.; Román, G.; Simonetti, S.; Ruiz, D.L. Removal of Paracetamol from Aqueous Solution by Activated Carbon and Silica. Experimental and Computational Study. *J. Contam. Hydrol.* **2021**, *236*, 103739. [CrossRef]
44. Sajid, M.; Bari, S.; Saif Ur Rehman, M.; Ashfaq, M.; Guoliang, Y.; Mustafa, G. Adsorption Characteristics of Paracetamol Removal onto Activated Carbon Prepared from Cannabis Sativum Hemp. *Alex. Eng. J.* **2022**, *61*, 7203–7212. [CrossRef]
45. Langmuir, I. The adsorption of gases on plane surfaces of glass, mica and platinum. *J. Am. Chem. Soc.* **1918**, *40*, 1361–1403. [CrossRef]
46. Dada, A.O.; Olalekan, A.P.; Olatunya, A.M.; Dada, O.J.I.J.C. Langmuir, Freundlich, Temkin and Dubinin–Radushkevich Isotherms Studies of Equilibrium Sorption of Zn^{2+} Unto Phosphoric Acid Modified Rice Husk. *IOSR J. Appl. Chem.* **2012**, *3*, 38–45. [CrossRef]
47. Romero-González, J.; Peralta-Videa, J.R.; Rodríguez, E.; Ramirez, S.L.; Gardea-Torresdey, J.L. Determination of Thermodynamic Parameters of Cr(VI) Adsorption from Aqueous Solution onto Agave Lechuguilla Biomass. *J. Chem. Thermodyn.* **2005**, *37*, 343–347. [CrossRef]

48. Ragadhita, R.; Nandiyanto, A.B.D. How to Calculate Adsorption Isotherms of Particles Using Two-Parameter Monolayer Adsorption Models and Equations. *Indones. J. Sci. Technol.* **2021**, *6*, 205–234. [CrossRef]
49. Tran, H.N.; You, S.-J.; Chao, H.-P. Thermodynamic Parameters of Cadmium Adsorption onto Orange Peel Calculated from Various Methods: A Comparison Study. *J. Environ. Chem. Eng.* **2016**, *4*, 2671–2682. [CrossRef]